Report title: Enhanced Activity of Nanocrystalline Zeolites for Selective Catalytic Reduction of NOx

Report type: Final Scientific/Technical Report

Start Date: 1/1/2006

End Date: 12/31/2006

Authors: Sarah C. Larsen, Vicki H. Grassian

Date Report Issued: March 30, 2007

DOE award number: DE-FG-06NT42739

Submitting Organization: University of Iowa, Iowa City, IA 52242

DISCLAIMER

ABSTRACT

Nanocrystalline zeolites with discrete crystal sizes of less than 100 nm have different properties relative to zeolites with larger crystal sizes. Nanocrystalline zeolites have improved mass transfer properties and very large internal and external surface areas that can be exploited for many different applications. The additional external surface active sites and the improved mass transfer properties of nanocrystalline zeolites offer significant advantages for selective catalytic reduction (SCR) catalysis with ammonia as a reductant in coal-fired power plants relative to current zeolite based SCR catalysts. Nanocrystalline NaY was synthesized with a crystal size of 15-20 nm and was thoroughly characterized using x-ray diffraction, electron paramagnetic resonance spectroscopy, nitrogen adsorption isotherms and Fourier Transform Infrared (FT-IR) spectroscopy. Copper ions were exchanged into nanocrystalline NaY to increase the catalytic activity. The reactions of nitrogen dioxides (NO_x) and ammonia (NH_3) on nanocrystalline NaY and CuY were investigated using FT-IR spectroscopy. Significant conversion of NO_2 was observed at room temperature in the presence of NH_3 as monitored by FT-IR spectroscopy. Copper-exchanged nanocrystalline NaY was more active for NO_2 reduction with NH_3 relative to nanocrystalline NaY.

Table of Contents

TITLE PAGE	**1**
DISCLAIMER	**2**
ABSTRACT	**3**
EXECUTIVE SUMMARY	**5**
REPORT DETAILS	
a. Experimental Methods	**6**
b. Results and Discussion	**7**
c. Conclusions	**11**
GRAPHICAL MATERIALS LIST	**12**
REFERENCES	**13**
LIST OF ACRONYMS AND ABBREVIATIONS	**14**
APPENDICES	**-**

EXECUTIVE SUMMARY

Nanocrystalline zeolites with discrete crystal sizes of less than 100 nm have different properties relative to zeolites with larger crystal sizes. Nanocrystalline zeolites have improved mass transfer properties and very large internal and external surface areas that can be exploited for many different applications. For example, nanocrystalline NaY with a crystal size of 23 nm has been synthesized in our lab with approximately 30% of the total surface area attributed to the external surface. Thus, the external surface of nanocrystalline zeolites can be utilized as an additional reactive or sorptive surface for catalytic applications. The additional external surface active sites and the improved mass transfer properties of nanocrystalline zeolites offer significant advantages for selective catalytic reduction (SCR) catalysis with ammonia (NH_3) in coal-fired power plants relative to current zeolite based SCR catalysts. Nanocrystalline NaY (15-20 nm) was synthesized and characterized using x-ray diffraction, nitrogen adsorption isotherms (surface area) and Fourier Transform Infrared (FT-IR) spectroscopy. Copper ions were exchanged into nanocrystalline NaY and the resulting material was characterized by electron paramagnetic resonance (EPR) spectroscopy. The reactions of nitrogen dioxide (NO_2) and ammonia (NH_3) on nanocrystalline NaY and CuY were investigated using FT-IR spectroscopy. Significant reaction of NO_2 was observed at room temperature in the presence of NH_3. Copper-exchanged nanocrystalline NaY was more active for NO_2 reduction with NH_3 relative to nanocrystalline NaY. Further spectroscopic studies are needed to more completely understand the mechanistic aspects of the SCR of NO_2 with ammonia on nanocrystalline zeolites.

REPORT DETAILS

a. Experimental Methods

Nanocrystalline Zeolite Synthesis The synthesis of nanocrystalline NaY has been described previously [1,2]. The original synthesis gel composition for zeolite Y was:

$$0.07Na: 2.4TMAOH: 1.0Al: 2.0Si: 132H_2O: 3.0i\text{-}PrOH:8.0EtOH$$

where TMAOH is tetramethylammonium hydroxide. Aluminumisopropoxide and tetraethylorthosilicate (TEOS) were used as aluminum and silicon sources, respectively, with isopropanol (*i*-PrOH) and ethanol (EtOH) as their respective hydrolysis products. The synthesis solution for zeolite Y was heated to 90 ºC in a glass flask containing a magnetic stirrer for 144 h for the first batch, and 48 h for later batches. After each batch, the zeolite crystals were recovered by centrifugation at 14,000 rpm for 30 min. After washing and drying, X-ray powder patterns and BET surface areas of the powders were measured to determine crystal structures and crystal sizes. The crystals are then calcined at 500^{o}C under oxygen flow for 16 hours to remove the TMAOH template.

The sodium in nanocrystalline NaY was exchanged with copper ions. For aqueous phase exchange, approximately 250 mg of nanocrystalline NaY was added to 0.05 M copper (II) nitrate and stirred overnight at room temperature[1]. The exchanged samples were washed twice with deionized water and centrifuge and then dried overnight at ~80°C. For the vapor phase exchange method[2], approximately 250 mg of synthesized nanozeolites (nanocrystalline NaY) and 25 mg of dry copper(I) chloride were ground together using a mortar and pestle. The solid mixture was then placed in a glass tube and exposed evacuated for 3 hours at room temperature and then at 400°C for 6 hours.

Elemental Analysis. A Perkin Elmer Plasma 400 Inductively Coupled Plasma atomic Emission Spectrometer (ICP/AES) spectrometer was used to determine the Si/Al ratio of the ZSM-5 samples. ZSM-5 samples were acid digested by dilute HF solution followed by neutralization in $NaBO_3$. Four standard solutions with known silicon (aluminum, sodium, copper) concentrations were prepared as calibration standards. Exact concentrations of silicon, aluminum, sodium and copper in the sample solution were obtained by projection from the working curve generated from standard solution data.

X-Ray Diffraction. A Siemens D5000 X-ray diffractometer with Cu Kα target and nickel filter was used to collect XRD powder patterns for the samples. XRD patterns were collected between 2θ angles of 5 and 55°.

Nitrogen Adsorption Isotherms. Nitrogen adsorption isotherms were obtained on a Quantachrome Nova 1200 multipoint BET apparatus using approximately 0.2 g sample for each measurement. Immediately prior to the N_2 adsorption, each sample was vacuum degassed at 120 °C for 1 hour. The specific surface area was measured by the BET method, which was performed automatically by the instrument. BET adsorption isotherms were collected for NaY samples before and after calcination to remove the template.

Electron Paramagnetic Resonance. Continuous wave electron paramagnetic resonance (EPR) spectra were acquired using a Bruker EMX61 EPR spectrometer equipped with a PC for spectrometer control and data acquisition. Typical EPR spectral parameters were: X-band frequency = 9.43 GHz, modulation amplitude = 0.5 G and modulation frequency = 100 kHz. The

magnetic field and microwave frequency were measured using a Hall probe and a frequency counter, respectively.

Fourier Transform-Infrared Spectroscopy. For FT-IR experiments, nanocrystalline NaY zeolite was mixed with water and sonicated for 30 minutes at room temperature[3]. The resulting hydrosol was coated onto a 3 cm × 2 cm tungsten grid held in place by nickel jaws. The nickel jaws were attached to copper leads so that the sample could be resistively heated. A thermocouple wire attached to the tungsten grid was used to measure the temperature of the sample. The tungsten grid with zeolite sample was placed inside a stainless steel cube. The cube had two BaF_2 windows for infrared measurements and was connected to a vacuum/gas handling system. The stainless steel IR cell was held in place by a linear translator inside the sample compartment of a Mattson Galaxy 6000 infrared spectrometer equipped with a narrowband MCT detector. The linear translator allowed each half of the sample grid to be moved into the infrared beam path. This allowed the detection of gas phase and adsorbed species in zeolites to be obtained under identical reaction conditions. Each absorbance spectrum shown was obtained by referencing 64 scans at an instrument resolution of 4 cm^{-1} to the appropriate background of the zeolite or the blank grid, unless otherwise noted. Reactant gases (NH_3 and NO_2) were loaded into the NaY zeolite through the gas handling system. Two absolute pressure transducers were used to monitor the pressure. The extinction coefficient of individual gases was calibrated using the characteristic IR absorption band and measuring the pressure using an absolute pressure transducer. Typically, the NaY zeolite was equilibrated with gas prior to a spectrum being recorded.

b. Results and Discussion

Synthesis and Transition Metal Ion Exchange. Approximately 2 g of nanocrystalline NaY was prepared using the synthetic method of recycling the synthesis solution as described previously[4, 5]. Four batches of nanocrystalline NaY were subsequently obtained from the same synthesis solution and were combined for catalytic studies. The average crystal size of the nanocrystalline NaY was 16 nm. The average external surface area was 252 m^2/g and the average total specific surface area was 511 m^2/g. Additional batches of nanocrystalline NaY were prepared for ion-exchange with copper.

The nanocrystalline NaY samples were exchanged with copper using two different methods: solution phase ion-exchange and solid state exchange. For solution phase ion-exchange, nanocrystalline NaY was added to an aqueous solution of $Cu(NO_3)_2$ and stirred for several hours. The sample was then centrifuged and dried in a drying oven. Powder x-ray diffraction of the sample before (bottom) and after ion-exchange (top) are shown in Figure 1. Some collapse of the zeolite structure (top) is observed in the XRD pattern which is significantly weaker than the parent NaY zeolite.

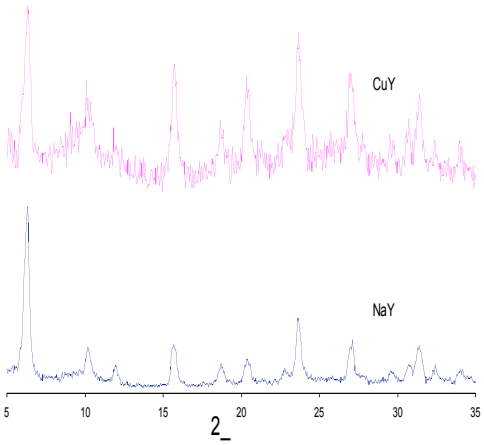

Figure 1: X-ray diffraction pattern of CuY before and after aqueous phase ion-exchange.

This loss of crystallinity was confirmed by a decrease in the specific surface area that was observed in nitrogen adsorption experiments after prolonged exposure of nanocrystalline NaY to water.

The nanocrystalline NaY samples were exchanged with copper using vapor phase exchange[6] so that contact with water would be minimized since the nanocrystalline NaY loses structural integrity with aqueous phase exchange. The nanocrystalline NaY was exchanged with copper using the following procedure. Approximately 250 mg of synthesized nanocrystalline NaY and 25mg of dry copper(I) chloride was ground together. The solid mixture was then placed in glass tube and exposed to vacuum system for evacuation. The solid was first evacuated at room temperature for 3 hours and then further evacuated at 400°C for 6 hours. The samples were characterized by powder X-ray diffraction (XRD) and electron paramagnetic resonance (EPR) spectroscopy.

XRD powder patterns of the NaY samples (Figure 2) were obtained before and after vapor phase exchange. Some broadening of the XRD pattern is observed for nanocrystalline NaY relative to Zeolyst NaY and this is due to line broadening that occurs as the crystal size becomes very small as expected. The crystal structure is intact after the vapor phase exchange as indicated by the XRD pattern at the top of figure 2. This is in contrast to the XRD pattern obtained after solution phase ion exchange which showed significant loss of crystallinity.

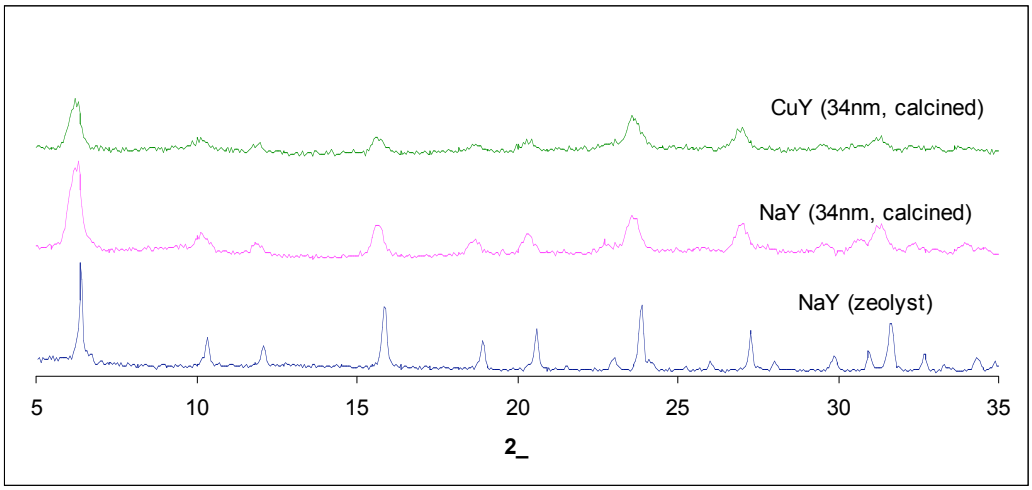

Figure 2: Powder X-ray diffraction pattern of commercial NaY from Zeolyst, synthesized nanocrystalline NaY and vapor-phase exchanged CuY.

The EPR spectra were collected for two different copper exchanged NaY samples at 77 K and are shown in Figure 3. Both samples were prepared by the vapor phase exchange method. The spectral parameters were obtained via spectral simulation using Bruker Simfonia software for CuY. The EPR parameters are $g_{\perp}$=2.058, $g_{//}$= 2.299, $A_{\perp}$=60 MHz, $A_{//}$=510 MHz, broadening (// 50G, $\perp$ 14 G), which are in good agreement with literature values for Cu-exchanged Y: $g_{\perp}$=2.054, $g_{//}$= 2.327, $A_{\perp}$=66 MHz, $A_{//}$=504.5 MHz.[1, 7, 8] These results suggest that the copper(II) species present in nanocrystalline CuY are hydrated, octahedral $[Cu(H_2O)_6]^{2+}$ or $[Cu(H_2O)_5OH]^{+}$ species. Cu(I) species may also be present but are not paramagnetic and are therefore not observed in the EPR experiment.

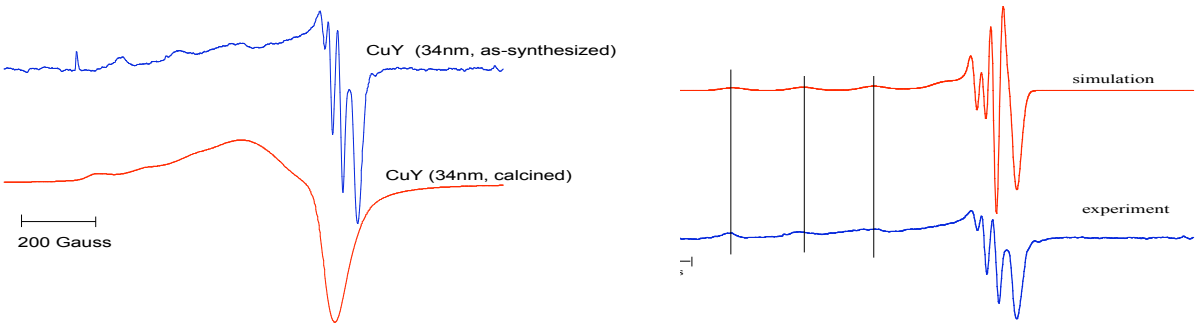

Figure 3. Experimental EPR spectra of copper-exchanged nanocrystalline Y (vapor phase method) (left hand side) and the simulated EPR spectrum for the CuY as synthesized sample.

FT-IR Investigation of the Reactivity of NO_2 and NH_3 on Nanocrystalline NaY. FT-IR studies were undertaken to investigate the reactivity of nanocrystalline NaY and nanocrystalline CuY for the selective catalytic reduction of NO_2 with ammonia. The surface species and gas phase species were monitored by FT-IR spectroscopy.

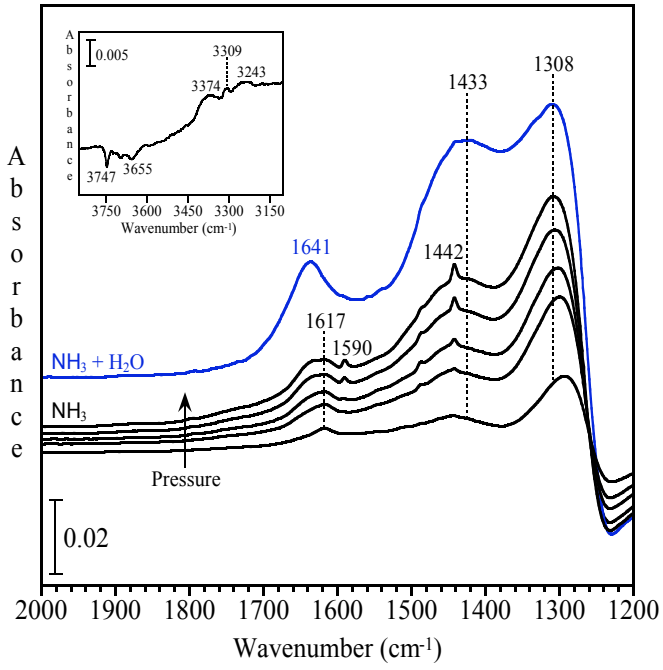

Figure 4. FT-IR spectra of ammonia adsorbed in nanocrystalline NaY at 298 K as a function of ammonia pressure (P = 0.05, 0.1, 0.2, 0.5 and 1 Torr). The inset displays the difference FT-IR spectrum in the O-H/N-H region following adsorption of 1 Torr NH_3 in nanocrystalline NaY at 298 K. The FT-IR spectrum of 1 Torr NH_3 and 1 Torr H_2O mixture adsorbed in nanocrystalline NaY at 298 K is also shown (in green). All spectra use the clean nanocrystalline NaY zeolite prior to

First the adsorption of ammonia on nanocrystalline NaY was monitored by FT-IR spectroscopy. The adsorption of ammonia (the proposed reductant in the SCR reaction) was probed using FT-IR spectroscopy. In the absence of water, NH_3 molecularly adsorbs in nanocrystalline NaY and can be identified by the absorption bands at 1308 cm^{-1} and 1617 cm^{-1} attributed to NH_3 bending mode of ammonia (Figure 4). NH_3 molecules adsorbed via hydrogen bonding with silanol groups of nanocrystalline NaY since the loss of silanol groups (3747 cm^{-1}) upon NH_3 adsorption was observed (Figure 4 inset). The loss of hydroxyl groups attached to EFAL sites (3655 cm^{-1}) is also observed, suggesting that NH_3 adsorption in part occurred on

EFAL sites. This is further supported by several absorption features between 1442 and 1590 cm^{-1} characterizing NH_3 adsorbed on Lewis acid sites that are associated with EFAL species in nanocrystalline NaY. The formation of ammonium ions in nanocrystalline NaY can be identified by the absorptions due to bending vibration at 1433 cm^{-1} (Figure 4) and stretching vibrations at 3374, 3309 and 3243 cm^{-1} (Figure 4 inset). The formation of ammonium ions can be resulted from the adsorption of NH_3 on Bronsted acid sites (hydroxyl groups attached to EFAL species).

In the spectra shown in Figure 4, the absorption band at 1433 cm^{-1} characterizing ammonium ions in the presence of water (1641 cm^{-1}) is much more intense relative to the absorption in the absence of water. The formation of ammonium ions upon adsorption of NH_3 and H_2O mixture must involve both the interaction between NH_3 and surface Bronsted acid sites and the reaction between NH_3 and H_2O (reaction 1).

$$NH_3 + H_2O \rightarrow NH_4^+ + OH^- \quad (1)$$

The formation of molecularly adsorbed NH_3 (1308 cm^{-1}) was not substantially influenced by the presence of water in the adsorption of 1 Torr NH_3 and 10 Torr H_2O in nanocrystalline NaY. This is due to the existence of Lewis acid sites and/or silanol groups in nanocrystalline NaY that are important sites for NH_3 adsorption.

The FT-IR spectrum of NO_2 exposed to nanocrystalline CuY is shown in Figure 5 and the presence of NO_2, N_2O_4, NO, and N_2O are observed in the gas phase. After exposure to NH_3 at room temperature, the FT-IR spectrum shows trace amounts of NO and N_2O, loss of NO_2 and production of H_2O. NH_4NO_2 is present and is seen in the gas phase post-SCR. The reaction of NH_4NO_2 to form N_2 and H_2O is shown below and has been reported in the literature previously[9] as a low temperature pathway to product N_2.

$$4NH_3 + 4NO + O_2 \rightarrow 4NH_4NO_2 \quad (2)$$

$$NH_4NO_2 \rightarrow N_2 + H_2O \text{ (low temperature)} \quad (3)$$

After adsorption of NO_2 (not shown), surface species (NO^+ and NO_3^-), surface species were observed on the zeolites and gas phase N_2O was also observed. Similar species are observed for analogous experiments on nanocrystalline NaY. The initial rates for the disappearance of NO_2 during NH_3-SCR over zeolite samples could be calculated using the FT-IR gas phase kinetic data. The results obtained at room temperature are listed in Table 1. These results indicate that the initial rate increases in the order: commercial NaY < nanocrystalline NaY < nanocrystalline CuY. This indicates that the nanocrystalline CuY has the highest initial and is ~40% more reactive under these conditions than commercial NaY.

Table 1. Initial rates for the disappearance of NO_2 during NH_3-SCR over zeolite samples at room temperature obtained from FT-IR data.

Zeolite Catalyst	Initial Rates ($\mu mol \cdot L^{-1} \cdot min^{-1} \cdot mg^{-1}$)	% Improvement over Commercial NaY
Commercial NaY	-0.50	0
Nano NaY	-0.70	29
Nano CuY	-0.83	40

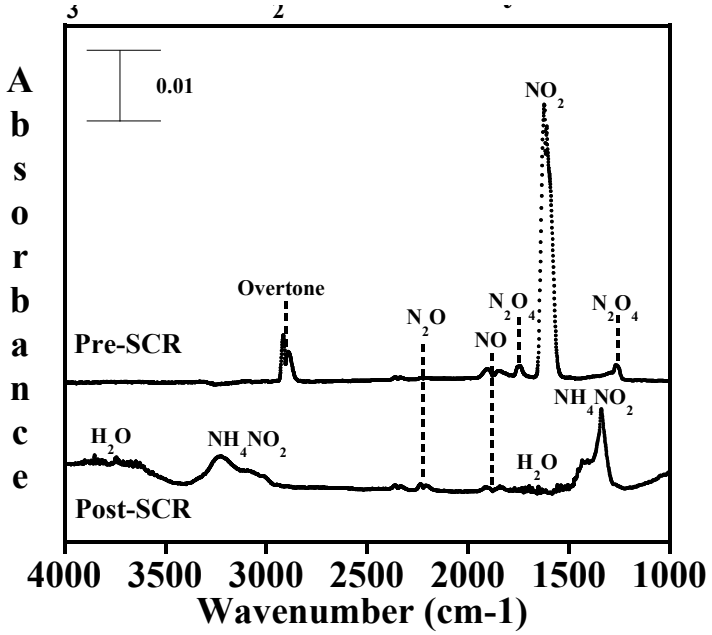

Figure 5. The FT-IR spectrum of nanocrystalline CuY before and after SCR of NO_2 with ammonia at room temperature.

c. Conclusions

Nanocrystalline NaY catalysts were synthesized, characterized and exchanged with the transition metal copper using a vapor phase exchange procedure to surmount the instability in water observed during typical aqueous exchange procedures. FT-IR spectroscopic studies indicated that NO_2 reacts readily with ammonia at room temperature and that the initial rate increases in the following order: commercial NaY < nanocrystalline NaY < CuY. The results suggest that nanocrystalline CuY has enhanced SCR reactivity with ammonia as the reductant. Future work will focus on understanding the role of the internal and external surface sites in the SCR reaction with ammonia, optimizing the copper exchange level for the SCR reaction, and comparing the reactivity of other transition metals (such as iron) in the nanocrystalline zeolites.

GRAPHICAL MATERIALS LIST

Figure 1: X-ray diffraction pattern of CuY before and after aqueous phase ion-exchange

Figure 2: Powder X-ray diffraction pattern of commercial NaY from Zeolyst, synthesized nanocrystalline NaY and vapor-phase exchanged CuY.

Figure 3. Experimental EPR spectra of copper-exchanged nanocrystalline Y (vapor phase method) (left hand side) and the simulated EPR spectrum for the CuY as synthesized sample.

Figure 4. FT-IR spectra of ammonia adsorbed in nanocrystalline NaY at 298 K as a function of ammonia pressure (P = 0.05, 0.1, 0.2, 0.5 and 1 Torr).

Figure 5. The FT-IR spectrum of nanocrystalline CuY before and after SCR of NO_2 with ammonia at room temperature.

REFERENCES

1. P.J. Carl and S.C. Larsen, Journal of Catalysis 182(1) (1999) 208.
2. C.A. Jones and S.C. Larsen, Catalysis Letters 78(1-4) (2002) 243.
3. G. Li, C.A. Jones, V.H. Grassian, and S.C. Larsen, Journal of Catalysis 234 (2005) 401.
4. W. Song, V.H. Grassian, and S.C. Larsen, Chemical Communications (23) (2005) 2951.
5. W.G. Song, G.H. Li, V.H. Grassian, and S.C. Larsen, Environmental Science & Technology 39(5) (2005) 1214.
6. V. Umamaheshwari, M. Hartmann, and A. Poppl, J. Phys. Chem. B 109 (2005) 19723.
7. P.J. Carl and S.C. Larsen, Journal of Physical Chemistry B 104(28) (2000) 6568.
8. J.C. Conesa and J. Soria, J. Magn. Res. 33 (1979) 295.
9. H.Y. Chen, Q. Sun, B. Wen, Y.H. Yeom, E. Weitz, and W.M.H. Sachtler, Catalysis Today 96(1-2) (2004) 1.

LIST OF ACRONYMS AND ABBREVIATIONS

SCR-selective catalytic reduction
EPR- electron paramagnetic resonance
FT-IR- Fourier transform infrared
XRD- x-ray diffraction
ICP/AES- inductively coupled plasma/atomic emission spectroscopy
BET-Brunauer-Emmett-Teller
TMAOH- tetramethylammonium hydroxide
TEOS- tetraethylorthosilicate
i-PrOH- isopropanol
EtOH-ethanol
NH_3-ammonia
NO_2-nitrogen dioxide
NO_x-nitrogen oxides (primarily a mixture of NO and NO_2)